PUBLICATION V

Micromechanical slow-velocity delay lines

In: Proc. 33rd European Microwave Conference,
Münich, Germany, 6–10 October, 2003. Pp. 967–970.

Micromechanical slow-velocity delay lines

Ari T Alastalo[1], Tomi Mattila[1], Heikki Seppä[1], James Dekker[2]

[1]VTT Information Technology, Microsensing, P.O. Box 1207, FIN-02044 VTT, Finland, Email: ari.alastalo@vtt.fi
[2]VTT Information Technology, Microelectronics, P.O. Box 1208, FIN-02044 VTT, Finland

***Abstract*— We consider a chain of coupled micromechanical resonators as a delay line for radio-frequency signals. Wave propagation in the chain is generated and detected using capacitive transducers. Analytical results, numerical simulations and rst measurements for the response of a prototype device are presented. The delay line is shown to have a bandpass response and a very low signal group velocity of the order of only few meters per second. Weaknesses of the rst prototypes are identi ed through simulations and a more optimal design is suggested.**

I. Introduction

Acoustic wave propagation in solids is an old and widely-studied topic. Typical applications, such as delay lines, filters and resonators, bear an analogy with the microwave electromagnetic devices [1]. Acoustic wave theory is extensively used e.g. in bulk-acoustic-wave (BAW) resonators and surface-acoustic-wave (SAW) filters. The recent advances in micro-electromechanical systems (MEMS) technology have opened the possibility for creating minituriased acoustical devices. As an example, a micromechanical resonator based on BAW-operation has been demonstrated to be well suited for creating a high spectral purity oscillator [2], [3]. Integrability with CMOS electronics as well as size reduction and power savings of MEMS components compared to off-chip solutions (such as SAW devices) facilitate design of efficient single-chip radio transceivers that could revolutionise wireless communication devices [4], [5].

In this paper we focus on a device geometry of a chain of coupled micromechanical resonators. Wave propagation along the chain is excited and detected using capacitive transducers. We present an analytical model for the device as well as numerical simulations and measurements for a first prototype device operating at 1.85MHz. The numerical simulations are done in Aplac® circuit simulator where both the mechanical resonators and the electronic circuitry of the measurement setup are modelled. It is shown, in particular, that reducing the feed-through capacitances to a minimum level is essential for good performance. Also dimensions of the resonator structures need to be carefully chosen, for example, to compensate for electrical spring softening introduced by the capacitive transducers. The first prototype device reported here does not reach sufficient performance but validates the analytical and numerical models. Improvements for the structure are suggested and will be concentrated on in future work. Furthemore, to reach higher frequencies the dimensions of the delay line need to be scaled down.

II. Prototype Delay Line

An IR spectroscope picture of a prototype spring-mass-chain delay-line structure is shown in Fig. 1. The device has been fabricated at VTT on a silicon-on-insulator (SOI) wafer having a device-layer thickness of 10μm. The silicon is heavily boron doped having a resistivity of $r \approx 2 \times 10^{-4}\Omega$m. The chain consists of 16 coupled tuning-fork elements that are released from the substrate below to vibrate in the plane of the picture. The tuning forks are identical and each of them has two beams of size 2.5μm$\times$100μm coupled at the ends of the beams and anchored to the surrounding structures by the vertical connects of size 2.5μm$\times$10μm. The size of the coupling connect between the tuning forks is 2.5μm$\times$5μm. The capacitive transducer pads at left and right ends of the chain have a size of 40μm$\times$75μm and are separated from the first and last tuning fork by a gap of size 0.5μm. The gap has to be made as small as possible in order to maximize the strength of the capacitive coupling (reaching gaps of size 0.1μm has been demonstrated [6]). The signal is brought to the capacitive transducer pads along the metallizations as shown in left and right edges of Fig. 1.

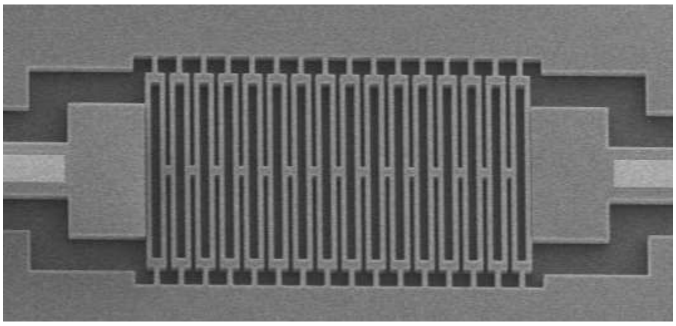

Fig. 1. IR microscope picture (top view) of a spring-mass-chain delay-line structure consisting of 16 coupled tuning forks. Length of the period in the chain is 12.5μm.

The fabrication process is illustrated in Fig. 2. Process begins with a SOI wafer having a 1μm buried oxide beneath a 10μm silicon device layer. After depositing a 1μm low temperature oxide on the wafer backside (a), an Al metallization is deposited and patterned on the front side (b). This metallization consists of a TiW diffusion barrier, 1μm Al, and a thin Mo top layer. Etching is carried out using either dry chlorine-based chemistry or wet etching. A short dip in Freckle etchant is used to remove the residual etch debris. Sawing lines are then patterned into the backside oxide and etched a few microns deep. The next step (c) is the patterning of the resonator structures, with nominal gaps of 0.5μm, and release holes with 1.5μm diameter. Inductively coupled plasma (ICP) etching is used to form the narrow gaps using the resist mask, which is then stripped in oxygen plasma before the backside sawlines are etched to a greater depth (d), again using ICP etching but with the previously patterned oxide as a mask. The buried oxide (and backside LTO) is then etched several minutes in 49% HF followed by drying in supercritical

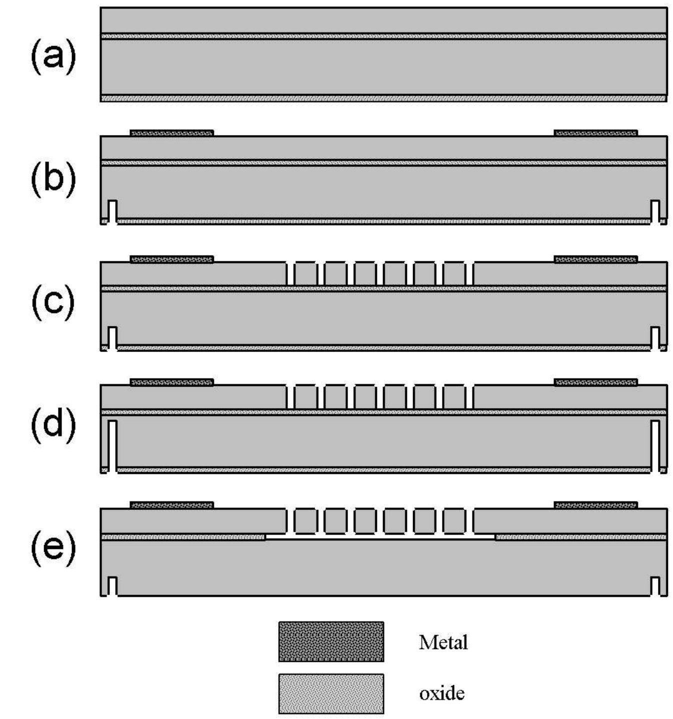

Fig. 2. MEMS device fabrication process. (a) Oxide deposition, (b) metallization, (c) device patterning, (d) sawline etching, (e) device releasing.

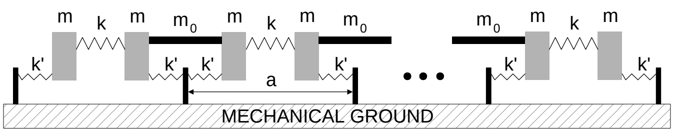

Fig. 3. Simplified model of the tuning-fork chain of Fig. 1.

CO_2 (e). The devices may be separated by cleaving along the sawlines or by sawing.

III. Analytical Model

At the frequency range of interest, each tuning fork can be modelled as two equal masses m connected to each other by a coupling spring k and anchored to walls with springs k'. The squared frequency ratio $(\omega_a/\omega_s)^2$ of the antisymmetric (masses moving with 180° phase difference) and symmetric (masses moving in phase) resonances of the tuning forks determines the ratio of the spring constants k and k':

$$k'/k = \frac{2}{(\omega_a/\omega_s)^2 - 1}. \tag{1}$$

If the masses coupling the consecutive tuning forks have a size of m_0, the chain can be modelled as shown in Fig. 3 without dissipation that can easily be included. Calculation of the dispersion relation for the anchored spring-mass chain of Fig. 3 is a straightforward generalization of the common text-book result for an unanchored chain [7]. Defining $K \equiv k'/k$ one finds for the center frequency $\omega_0 = 2\pi f_0$, bandwidth $\Delta\omega = 2\pi\Delta f$ and signal group velocity in the center of the passband v_g of the chain:

$$\begin{aligned}
\omega_0 &= \sqrt{\frac{2k}{2m+m_0}}\sqrt{K+1} \\
\Delta\omega &= \sqrt{\frac{2k}{2m+m_0}}\left(\sqrt{K+2}-\sqrt{K}\right) \\
v_g &= \frac{a}{2}\sqrt{\frac{2k}{2m+m_0}}/\sqrt{K+1}\ ,
\end{aligned} \tag{2}$$

where a is the length of the period of the chain. For the structure in Fig. 1 we have $a = 12.5\mu$m, and assume $k' = 258$N/m, $k = 33.5$N/m, $m = 2.1\times10^{-12}$kg, and $m_0 = 2.91\times10^{-13}$kg. Parameters k', k and m have been approximated based on FEM simulations with ANSYS® and with the well known results for vibrating beams [8] using an isotropic approximation for the SOI material with Young's modulus $Y = 130$GPa and density $\rho = 2330\text{kg/m}^3$. The coupling mass m_0 is taken as the dimensional mass of the connect. One finds with (2) $f_0 \approx 1.8$MHz, $\Delta f \approx 210$kHz and $v_g \approx 8.2$m/s. Result (2) furthermore shows that increasing the strength of the anchoring spring k' with respect to the coupling spring k increases the center frequency while decreasing both bandwidth and group velocity.

IV. Measurement and Simulation Results

Measurement of the S_{21} for the delay line has been done with HP4195A network analyser. The MEMS device and a JFET preamplifier were placed in a vacuum chamber having a 0.001bar pressure. The circuit diagram of the measurement setup is shown in Fig. 4 with the preamplifier modelled by measured input capacitance and resistance. The resonator chain and the capacitive signal connects have been modelled with the MEMS transducer and resonator components of Aplac. Noise has not been included in the simulations. The center frequency and bandwidth expected based on the analytic calculation above is in relatively good agreement with the measured response of Fig. 5. Furthermore, as shown in Fig. 6 the Aplac simulation produces essentially the same result that has been measured. The absolute level of S_{21} has been removed in the measurement by calibrating the network analyser with zero bias voltage. Here C_{thr} has been measured for the device, $(\omega_a/\omega_s)^2$ is obtained through FEM simulations, and Q is selected based on measured properties of single tuning-fork resonators.

It is found that the main reasons for suboptimal performance in Fig. 5 are the feed-through capacitance C_{thr}, too low bias voltage and electrical softening of the first and last springs in the chain introduced by the capacitive transducers. Improving on these issues leads to significantly better performance as suggested by the simulation results of Fig. 7 where also the resulting group delay has been shown. In particular, we have reduced the feed-through capacitance to 1fF, increased the bias voltage close to its limits to $U_{\text{dc}} = 35$V (76% of the pull-in voltage), and canceled the electrical spring softening in the first and last tuning fork. Compensation for the electrical spring softening by strengthening the first and last springs is critical for optimum signal coupling to the line. The reduction of the feed-through capacitance has a smaller effect on the dynamic range and pass-band ripple of the device. The feed-through capacitance can be reduced, for example, by using a differential readout amplifier as suggested in [9]. The ripple in the passband response and in the group delay can be further

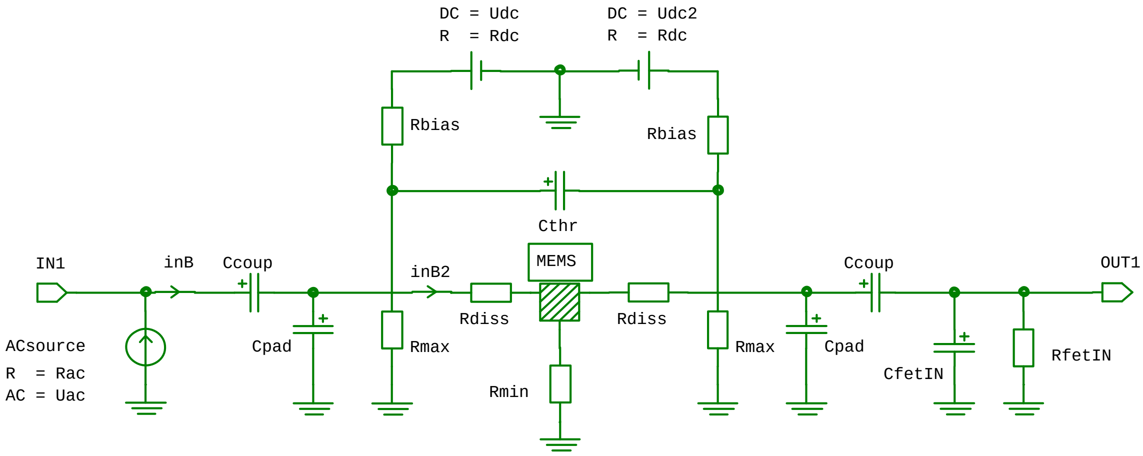

Fig. 4. Circuit diagram used in the Aplac simulation of the measurement setup. Here symmetric bias has been used ($U_{dc} = U_{dc2}$), and $R_{ac} = R_{dc} = 50\Omega$, C_{coup}=100nF, $C_{pad} = 0.3$pF and $R_{bias} = 10\text{M}\Omega$. The input capacitance and resistance of the measurement preamplifier are C_{fetIN} =6pF, $R_{fetIN} = 10\text{M}\Omega$.

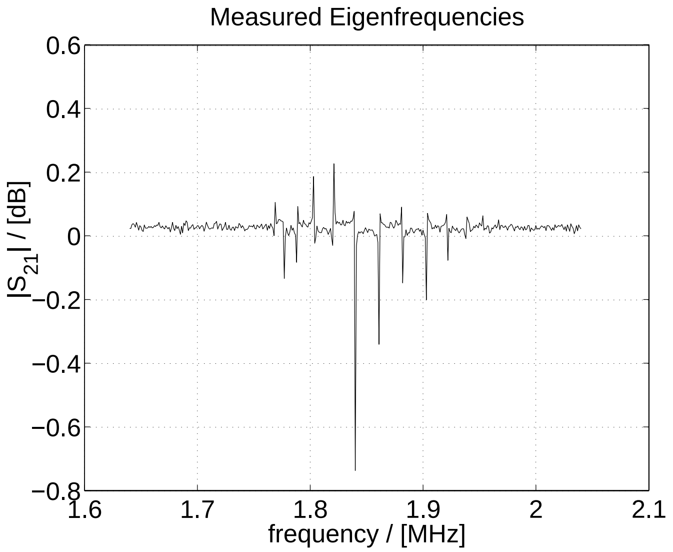

Fig. 5. Measured amplitude response of the device of Fig. 1 with 15V bias voltage and 0dBm signal level. Calibration of the network analyser is done with 0V bias.

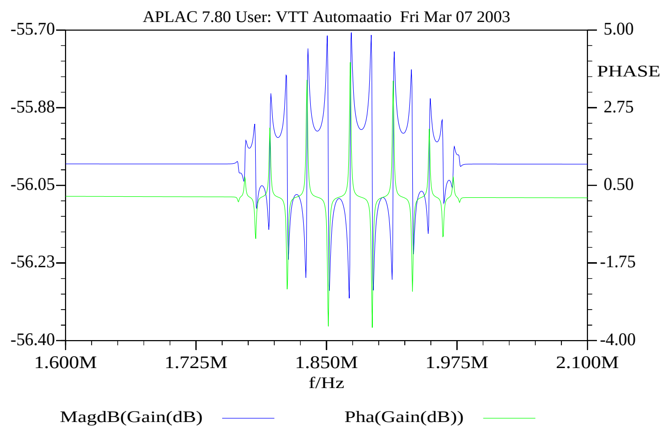

Fig. 6. Simulated voltage gain V_{out}/V_{in} corresponding to the measurement in Fig. 5 with $C_{thr} = 10$fF, $U_{dc} = 15$V, $Q = 10^3$, $N = 16$, $(\omega_a/\omega_s)^2 = 1.26$, and $R_{diss} = 0$. Values of C_{thr} and Q are measured for the device on Fig. 5. The frequency ratio $(\omega_a/\omega_s)^2$ is obtained through FEM simulations. Parameters of the model in Fig. 3 are as stated in text below (2).

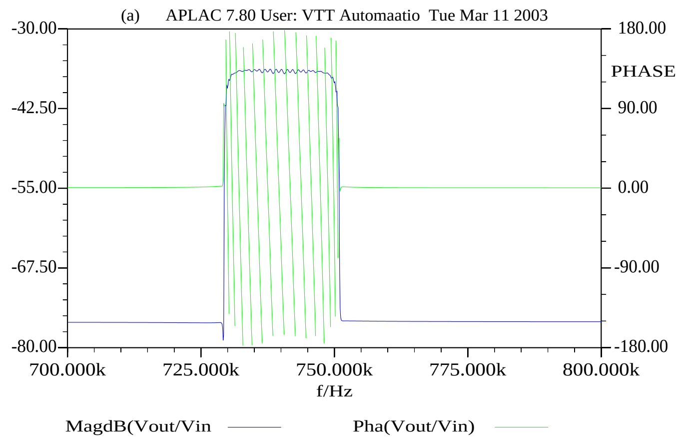

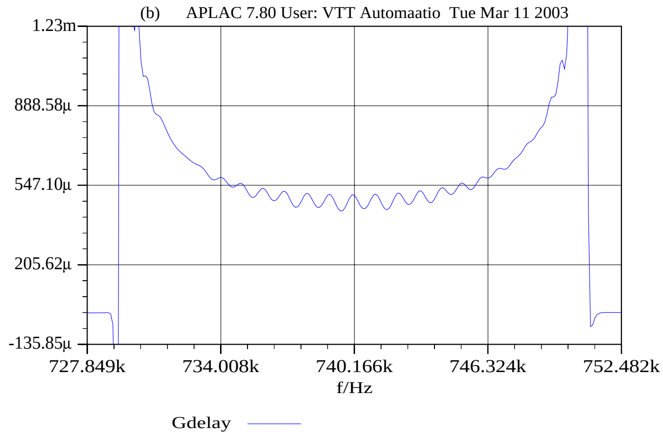

Fig. 7. (a) Simulated V_{out}/V_{in} in a measurement setup of Fig. 4 for a structure where extra masses of m_0 =2.5e-11kg are added between the tuning forks with $(\omega_a/\omega_s)^2 = 1.06$ and $Q = 10^4$ in a chain of $N = 32$ (period of the chain is now 25μm). Half of the extra mass is added before the first and after the last tuning fork in the chain. Furthermore, bias voltage is set to $U_{dc} = 35$V, feed-through capacitance is reduced to $C_{thr} = 1$fF, and resistors of $R_{diss} = 1\text{M}\Omega$ are used to reduce the quality factor (smooth out the resonances of the chain). The first and last tuning-fork springs are strengthend to cancel the electrical softening. For the rest of the chain we have (see Fig. 3) $k' = 307$N/m, $k = 9$N/m and $m = 2.1 \times 10^{-12}$kg. (b) Group delay in seconds through the structure considered in (a). At the passband center the delay is 450μs corresponding to signal group velocity of 1.8m/s. The simulated results are in agreement with (2).

reduced by increasing the number of the periods in the chain, increasing the electrical dissipation R_{diss} and decreasing the bandwidth by strengthening the achoring springs as discussed above.

The characteristic impedance level of the MEMS transmission line can conveniently be probed in Aplac simulations. With 0.5μm transducer gaps, the impedance level varies accross the passband in the few-megaohms range. Reducing the transducer gap is an effective solution to reach significantly lower impedances. Namely, the characteristic impedance depends on the gap as $Z \propto d^4$ while the depence on other parameters, such as resonator mass (m), spring constant (k), transducer area (A) and bias voltage (U_{dc}), is at most of the second order. In fact, the result for the characteristic impedance of bulk-acoustic rod wavequides in [10] ($Z = d^4\sqrt{\rho E}/(A(\varepsilon_0 V)^2)$, where E and ρ are the Young modulus and density of the rod material, respectively) roughly generalizes to the current situation when the mechanical characteristic impedance of the rod $A\sqrt{\rho E}$ is replaced by $\sqrt{km}$ (see Fig. 3). Furthermore, comparing to [10], it is found that the characteristic impedance of the spring-mass chain typically is several orders of magnitude lower than the rod-wavequide values. Thus the spring-mass-chain approach can provide a more feasible realization for a MEMS delay line when the needed operation frequency is not too high. Among other possible solutions to reduce the impedance level of MEMS delay lines is to use inductive coupling instead of the capacitive transducers. This, however, would require an external magnetic field.

V. Conclusion

We have described a MEMS structure where mechanical wave propagation with extremely low velocity can be used for signal trasmission to construct a delay line reaching high delays without digital signal processing. Future work focuses on optimizing the performance of the line and on reducing the gap as well as the vibrating dimensions of the structure in order to reach higher frequencies and lower characteristic impedances of the delay line.

Acknowledgement

This work is supported by the Academy of Finland (grant 20542).

References

[1] B. A. Auld, *Acoustic Fields and Waves in Solids*, 2nd ed., Krieger, 1990.

[2] T. Mattila, J. Kiihamäki, T. Lamminmäki, O. Jaakkola, P. Rantakari, A. Oja, H. Seppä, H. Kattelus, and I. Tittonen, “A 12 MHz Bulk Acoustic Micromechanical Oscillator,” *Sensors and Actuators A: Physical*, vol. 101, pp. 1–9, Sept. 2002.

[3] Ville Kaajakari, Tomi Mattila, Aarne Oja, Jyrki Kiihamäki, Hannu Kattelus, Mika Koskenvuori, Pekka Rantakari, Ilkka Tittonen, and Heikki Seppä, “Square-Extensional Mode Single-Crystal Silicon Micromechanical RF-resonator,” in *Proc. Transducers´03*, June 8–12, 2003.

[4] Clark T.-C. Nguyen, “Frequency-Selective MEMS for Miniaturized Low-Power Communication Devices,” *IEEE Trans. Microwave Theory Tech.*, vol. 47, no. 8, pp. 1486–1503, Aug. 1999.

[5] J Jason Yao, “RF MEMS from a device perspective,” *J. Micromech. Microeng.*, vol. 10, pp. R9–R38, 2000.

[6] Wan-Thai Hsu, John R. Clark, and Clark T.-C. Nguyen, “A Sub-Micron Capacitive Gap Process for Multiple-Metal-Electrode Lateral Micromechanical Resonators,” in *Proc. IEEE MEMS Conference*, Interlaken, Switzerland, 2001, pp. 349–352.

[7] Neil W. Ashcroft and N. David Mermin, *Solid State Physics*, Saunders College Publishing, 1976.

[8] Warren C. Young, *Roark’s Formulas for Stress and Strain*, McGraw-Hill, 1989.

[9] P. Rantakari, J. Kiihamäki, M. Koskenvuori, T. Lamminmäki, and I. Tittonen, “Reducing the Effect of Parasitic Capacitance on MEMS Measurements,” in *Proc. Transducers´01*, June 8–12, 2001.

[10] Ari T. Alastalo, Tomi Mattila, and Heikki Seppä, “Analysis of a MEMS Transmission Line,” to appear in: *IEEE Trans. Microwave Theory Tech.*, vol. 51, no. 8, Aug. 2003.